ORIGINAL PAPER

Production and characterization of sustainable biocompatible PLA/walnut shell composite materials

İdris Karagöz[1]

Abstract

Various treatments, such as alkaline and silane treatments, are commonly applied to natural fillers before production to enhance their quality, thermal stability, and water absorption capacity and improve the fiber–matrix interface properties. However, these processes are not environmentally friendly and may escalate the production cost of composites due to the need for additional processing steps in mass production. This study delves into the impact of untreated walnut shell (WS) filler material, employed in varying ratios (ranging from 10 to 40%) as a filler, on the mechanical, thermal, morphological, and physical properties of environmentally friendly poly-lactic acid (PLA) matrix composites. The experimental results highlight a significant decrease in tensile modulus by 28%, tensile strength ranging from 32 to 65%, a decrease in flexural modulus by 22%, and flexural strength ranging from 24 to 58% with varying WS filler ratios. Time-dependent water absorption and increased density were observed. FT-IR analysis indicates structural similarities, while DSC results show minimal effects on glass transition temperature and crystallinity. TGA results reveal reduced thermal stability with increasing WS content. SEM microstructure imaging demonstrates homogeneous WS particle distribution, but higher WS content leads to increased brittleness and diminished resistance properties. In conclusion, this study underscores the importance of balancing sustainability through WS filler ratios while preserving mechanical performance.

Keywords Biocomposite · Natural fibers · Mechanical properties · Injection molding

✉ İdris Karagöz
idris.karagoz@yalova.edu.tr

1   Department of Polymer Materials Engineering, Faculty of Engineering, Yalova University, 77200 Yalova, Turkey

🖄 Springer

Introduction

Sustainability can be defined as the enduring capacity to replace resources without necessitating new ones, considering the well-being of both society and individuals in the processes of production and consumption, while also preventing harm to the environment. As natural resources deplete at an alarming rate on a global scale, coupled with increasing environmental concerns, the production of sustainable and recyclable products has emerged as a paramount focus for environmentalists and professionals in the manufacturing sector in recent years. Notably, addressing the challenge of plastic waste has spurred a heightened interest in utilizing eco-friendly materials alongside polymers [1]. These initiatives present a significant opportunity to mitigate the adverse environmental impact of polymers and improve the overall quality of life for future generations [2].

Polylactic acid (PLA) stands out as an environmentally friendly polymer due to its biodegradable, renewable, and biologically sourced properties. The biodegradability of PLA relies on its ability to be metabolized by microorganisms in nature, rendering it harmless to the environment. However, this degree of biodegradability can vary depending on PLA's stereochemistry, environmental conditions, and the context in which PLA is situated [3]. It is a thermoplastic polymer produced from lactic acid monomers obtained through the polymerization of starch-based plant raw materials, such as corn, potatoes, sugar beets, and sugarcane. These eco-friendly characteristics have captured the interest of researchers and industries, positioning PLA as a viable alternative to traditional plastics in various applications. PLA's biodegradability ensures its decomposition in nature without causing harm to the environment after use. Furthermore, its derivation from renewable sources makes it a more sustainable option compared to petrochemical-based polymers. Since PLA is produced using biological resources, it also contributes to reducing greenhouse gas emissions associated with fossil fuel usage. In conclusion, the eco-friendly attributes of PLA and its role in sustainability have spurred increased research interest in developing environmentally friendly and sustainable materials for the plastic industry and other applications. These efforts aim to address the issue of plastic waste and create a more sustainable world for future generations. Despite its advantages, PLA has limitations, such as low density, low-temperature flammability, and a lower melting point. These characteristics may render PLA unsuitable for applications requiring high temperatures [4]. Additionally, PLA might lack sufficient mechanical properties for certain applications that demand hardness and impact resistance. Consequently, its performance can be enhanced by reinforcing it with various filler materials. In recent years, there has been a growing prominence in using natural fiber agricultural wastes as filler materials in composite technologies [5]. Various fibers and fillers, including cellulose [6, 7], rice straw [8, 9], flax [10], wood flour [11], oak sawdust [12], bagasse fiber [13], eggplant stems [14], hazelnut shells [12, 15–20], walnut shells (WS) and sunflower husks [20], almond shells [21], cocoa shells [22, 23], eucalyptus fiber [24], sugarcane [25], and more, have been utilized to achieve higher thermal and mechanical properties. Hybrid composites,

combining inorganic and different organic additives, such as SEBS [26], coal powder [27], basalt [28], calcium carbonate ($CaCO_3$), perlite, potassium dichromate ($K_2Cr_2O_7$) [17], glass fiber [18], mica, kaolin, mica, wollastonite, silica, graphite [29], and various other additives [7–24], have been produced to further enhance PLA's properties.

The utilization of natural fibers presents an opportunity to enhance the biodegradability of bio-based polymers like PLA, which, despite being a biopolymer, exhibits relatively low biodegradability compared to other biopolymers. This utilization also helps in reducing reliance on non-biodegradable polymers, thus creating environmentally friendly alternatives [1]. In a study conducted by Barczewski et al. [1], walnut shells, hazelnut shells, and sunflower husks were employed as filler materials in varying proportions (15%-35%). The researchers noted that the introduction of natural filler materials had a discernible impact on the mechanical properties of the composites. The incorporation of powdered fillers, such as walnut shell and hazelnut shell, led to improvements in hardness and resistance in the epoxy composite. Conversely, the addition of sunflower husks increased the viscosity of the composite, resulting in a porous structure that compromised the mechanical performance. In another study by Orue et al. [30], PLA-based biocomposites were prepared with varying amounts of walnut shell flour and 10% by weight of epoxidized linseed oil. An alkali treatment applied to the walnut shell proved effective in removing non-cellulose components, enhancing thermal stability and crystallinity. Furthermore, this treatment improved adhesion between PLA and WS, positively influencing tensile strength.

In recent years, the growing interest in environmentally friendly and sustainable products has extended its influence to 3D printing technologies. A notable trend in this realm is the development of 3D printer filaments using PLA-based bio-waste fillers [4]. In a study by Umerah et al. [31], a remarkable 50% increase in tensile strength was reported with a 0.6% filler ratio when filaments were produced using carbon nanoparticles derived from coconut shells. Similarly, in a study where WS flour and epoxidized linseed oil were employed to plasticize PLA-based biocomposites, an alkaline treatment was found to significantly enhance tensile strength and improve thermal stability [30]. Various studies have delved into the incorporation of additives such as marble powder [32], hemp, marijuana, rosemary, carrots, and tomatoes [33, 34], coconut fiber, coconut shell powder [35], mushroom powder [36], palm fiber [37], rice straw powder [38], rice husk, wood powder, and bagasse particles [39] to formulate polymer composites and filaments.

WS, due to its inherent properties in conjunction with processes like alkaline and silane treatments, has the potential to enhance the characteristics of composite materials when added to a PLA matrix. However, these additional processes significantly increase the production costs of composites. This study investigates the impact of using untreated walnut shell fillers in different proportions as fillers in PLA matrix composites, examining their effects on composite properties. The study explores the mechanical, thermal, and morphological effects of walnut shell fillers on PLA composites. The aim of this research is to enhance our understanding of developing economical, sustainable, and environmentally friendly composite materials through a suitable combination of PLA and organic fillers and to evaluate

potential applications in future practices. Ultimately, materials obtained by incorporating organic fillers into PLA composites could offer eco-friendly alternatives that may replace traditional polymers. The use of such composite materials may contribute to solutions for waste management issues, mitigating the adverse environmental impacts of the plastic industry and promoting a sustainable future.

Materials and methods

Materials

The PLA/WS compounds were investigated experimentally using the biopolymer Ingeo Biopolymer 4032D, which has a density of 1.24 g/cm^3 and a melting temperature ranging from 155 to 170 °C, as the matrix material. WS (density of 1.0–1.2 g/cm^3) from Maraş18 variety walnuts grown in the Çağlayancerit district of Kahramanmaraş was chosen as the filler material. The WS consists of two distinct parts: a sturdy outer woody shell and a softer internal barrier. For this study, only the robust outer shell portion of the WS was isolated and utilized.

Preparation of PLA/WS Compounds and test samples

It is known from the literature that as particle size decreases, higher mechanical properties are obtained, and smaller particle sizes are generally preferred in studies [40, 41]. The WS was ground using a crusher/grinder mill (Lavion HC-500Y Brand). The powdered WS, which consisted of particles with a very broad distribution that could negatively impact the mechanical properties of the envisioned compounds, was sieved using a sieve machine to obtain WS powders with a narrower distribution. In order to achieve both a homogeneous distribution and considering the proportions of particle size distributions obtained after the grinding process, the particle size was determined as < 100 microns.

WS, like other cellulose-containing materials, is highly sensitive to moisture and water. Therefore, the powdered WS was dried in an oven at 100 °C for two hours before being mixed with PLA in the extruder. Following the crushing and sieving process, the materials were prepared according to the mixing ratios provided in Table 1 by weighing them using a precision scale. Initially, all the ingredients added to a bucket underwent a mechanical stirring process for 10 min. After the

Table 1 Mixing ratios used in the study	Code	PLA (%)	WS (%)	Plasticizer (%)
	PLAWS00	100.00	–	–
	PLAWS10	89.95	10	0.05
	PLAWS20	79.90	20	0.10
	PLAWS30	69.85	30	0.15
	PLAWS40	58.80	40	0.20

mechanical stirring process, the samples were drawn into filament form using an extruder equipped with a special mixing screw from the Robodigg brand, employing the melt blending method. In the preparation of the mixtures, glycerin, added at a ratio of 0.05%, served as a plasticizer for each 10% of WS in the mixture. Following this, the filament-shaped materials were granulated with the assistance of a granulator. Tensile and impact specimens, derived from mixtures in granule form, were then manufactured using the Engel Spex brand injection machine, adhering to the ISO 294 standard. The parameters were set at 80 bar injection pressure, 50 mm/s injection speed, 55 bar holding pressure, and a 35-s cycle time. The process from the production to the characterization of PLA/WS composites is illustrated in Fig. 1.

Characterization

The tensile test was conducted at room temperature with a Zwick Z020 Model testing machine equipped with a 20 kN load cell, following the ASTM D638 standard, at a pulling rate of 50 mm/min. The three-point bending test was performed on the same testing machine using a compression fixture, according to the TS EN ISO 178 standard, at room temperature and a bending rate of 2 mm/min. The impact test, in accordance with ASTM D256, was carried out using a 5.5 J hammer on an Instron 120D Model testing machine. Hardness testing was conducted according to the ASTM D2240 standard using the Shore D scale and Loyka M01D brand analog durometer. Ten measurements were taken for each sample, and the hardness value was determined as the Shore D hardness by calculating the arithmetic mean of these measurements.

The density of PLA/WS composites was measured using the liquid pycnometer method in accordance with ISO 1183. Prior to measurement, the pycnometer was
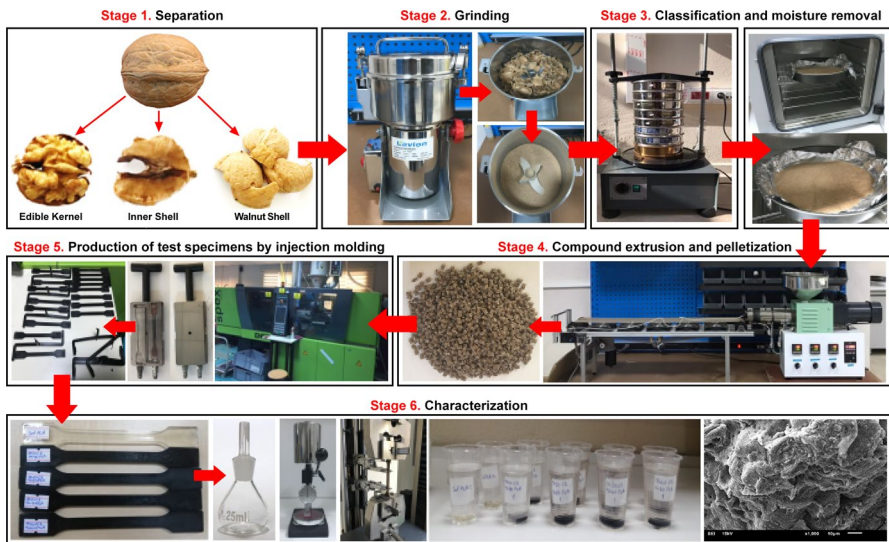

Fig. 1 The process from the production to the characterization of PLA/WS composites

dried at 25 °C, and its weight was determined. Subsequently, samples initially ground to a size of 200 μm were added to the pycnometer, approximately filling 1/4 of it, and weighed to determine their weight, which was then recorded. The pycnometer was then slowly filled with distilled water, intermittently shaken to eliminate air bubbles between particles. The weight was determined after filling, and the same process was repeated for the pycnometer without the samples to be used for density calculation. To prevent deviations due to experimental errors, three measurements were taken for each sample. The calculation of density utilized Eq. 1, where A represents the empty weight of the pycnometer bottle and cap, B represents the weight of the pycnometer bottle, cap, and composite samples before adding distilled water, C represents the weight of the pycnometer bottle, cap, and composite samples after adding distilled water, and D represents the weight of the pycnometer bottle and cap after being filled with distilled water. The symbol ρ in the equation represents the specific gravity of the distilled water used (1).

$$\text{Density} = ((B/A)/((D - A) - (C - B))) \times \rho \qquad (1)$$

The weights of samples, cut into rectangular shapes with dimensions of $4 \times 20 \times 30$ mm for the water absorption test, were measured to determine the initial weight. Subsequently, the samples were placed in the test container, completely submerged in water, and subjected to the water absorption process. After the initial one-hour period, the materials were removed from the container with tweezers. To remove excess water from the sample surfaces, a drying process was performed using paper towels without applying pressure. Then, the samples were weighed, and the amount of water absorption was calculated using the equation provided in Eq. 2. The same procedures were repeated after 2, 3, 5, 12, 24, 72, 96, 168, 192, 216, and 240 h.

$$\text{Water Absorption} = \left(\frac{\text{Final weight} - \text{Inital weight}}{\text{Inital weight}} \right) \times 100 \qquad (2)$$

FT-IR tests were conducted on a PerkinElmer Spectrum 100 FT-IR instrument, following the ASTM D6348 standard, in the wavelength range of 4000 cm^{-1} to 400 cm^{-1}. To observe the thermal transitions of PLA/WS composites, thermal properties were examined using differential scanning calorimetry (DSC, Seiko DSC 7020 Model) in accordance with the ASTM D3417 standard. The heating rate was set at 10 °C/min under a nitrogen atmosphere. The crystallinity degree (Xc) of PLA was calculated using Eq. 3. Here, ΔHm represents the melting enthalpy directly obtained by DSC, ΔHcc is the cold crystallization enthalpy, ΔH°m is the enthalpy of melting for 100% crystalline polymer (93 J/g for PLA), and ϕi is the mass fraction of PLA in the sample [42]. DSC analysis was also employed to investigate the effect of walnut shell addition on the glass transition temperature (Tg), cold crystallization temperature (Tcc), and melting temperature (Tm) of the samples. Thermogravimetric analysis (TGA) was performed using a Seiko Exstar TG/DTA 6300 under a nitrogen flow. The PLA/WS composite samples were heated up to 600 °C with a heating rate of 10 °C/min.

$$Xc = \left(\frac{\Delta Hm - \Delta Hcc}{\Delta H°m \times \phi i} \right) \times 100 \qquad (3)$$

The morphology of the fractured surfaces of materials obtained from the impact test was investigated using the Inspect S50 Model scanning electron microscope (SEM). The samples were coated with 100 Å gold under vacuum to achieve an inert and conductive surface, and the microstructures were photographed under a voltage of 20 kV.

Results and discussion

Tensile test results of PLA/WS composites

The tensile test results are presented collectively in Table 2, with their graphical comparison illustrated in Fig. 2. As the content of walnut shell in PLA composites increases, the tensile strength of the PLA composite decreases. While pure PLA (PLAWS00) exhibits a high elastic modulus (1950 MPa ± 27), tensile strength (65.0 MPa ± 1.0), and elongation at break (4.3%), a notable decrease in these properties is observed with the increasing addition of walnut shell content to the structure. PLA samples with 10%, 20%, 30%, and 40% walnut shell show a reduction in elastic modulus, tensile strength, and elongation at break, respectively. These results indicate that the addition of walnut shell in mixtures, without the use of any compatibilizing or reinforcing material, adversely affects the durability and flexibility of the material. In applications where tensile properties are crucial, the interface and adhesion between the matrix and the fibers can be enhanced by applying an alkaline treatment to the WS [29]. As a result, tensile strength and elastic modulus can be increased.

Three-point bending test results of PLA/WS composites

The results of the three-point bending test are presented collectively in Table 3, and their graphical representation is shown in Fig. 3. Generally, the three-point bending test results for PLA materials modified with walnut shell additive indicate a negative trend in bending performance as the additive ratio increases. While pure PLA

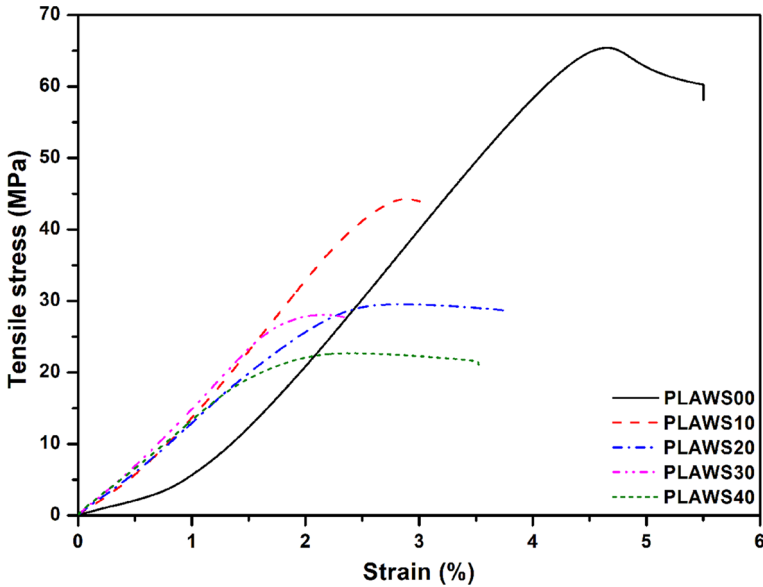| Table 2	The tensile test results	Code	Tensile elastic modulus (MPa)	Tensile strength (MPa)	Elongation (at break) (%)
		PLAWS00	1950 ± 27	65.0 ± 1.0	4.3
		PLAWS10	1950 ± 53	44.0 ± 1.2	2.9
		PLAWS20	1450 ± 20	29.6 ± 0.4	2.8
		PLAWS30	1740 ± 46	28.8 ± 1.4	2.1
		PLAWS40	1400 ± 21	22.4 ± 0.6	2.4

Fig. 2 Graphical comparison of tensile test results for PLA/WS composites

Table 3 The three-point bending test results

Code	Flexural elastic modulus (MPa)	Flexural strength (MPa)	Elongation (%)
PLAWS00	3480 ± 12.5	109.0 ± 0.70	4.4
PLAWS10	3460 ± 40.4	79.7 ± 0.97	3.1
PLAWS20	2690 ± 62.1	52.9 ± 3.47	3.0
PLAWS30	3150 ± 60.6	49.4 ± 2.05	2.1
PLAWS40	2690 ± 124	44.8 ± 1.86	2.6

(PLAWS00) demonstrates a high elastic modulus (3480 MPa ± 12.5) and flexural strength (109.0 MPa ± 0.70), a significant decrease in these properties is observed with an increase in the amount of additive. In 10% walnut shell additive PLA (PLAWS10), the elastic modulus remains relatively constant, but flexural strength and elongation at break decrease. The 20%, 30%, and 40% walnut shell additive PLA samples exhibit further decreases in elastic modulus, flexural strength, and elongation at break, respectively. These results indicate that the walnut shell additive adversely affects the material's bending strength and flexural elastic modulus, demonstrating lower performance compared to pure PLA. By modifying the different particle sizes incorporated into the composite, flexural strength can be enhanced [2, 4, 23]. Currently, PLA/WS composites produced in this manner can be utilized in the manufacturing of interior components for vehicles due to their lightweight nature [23].
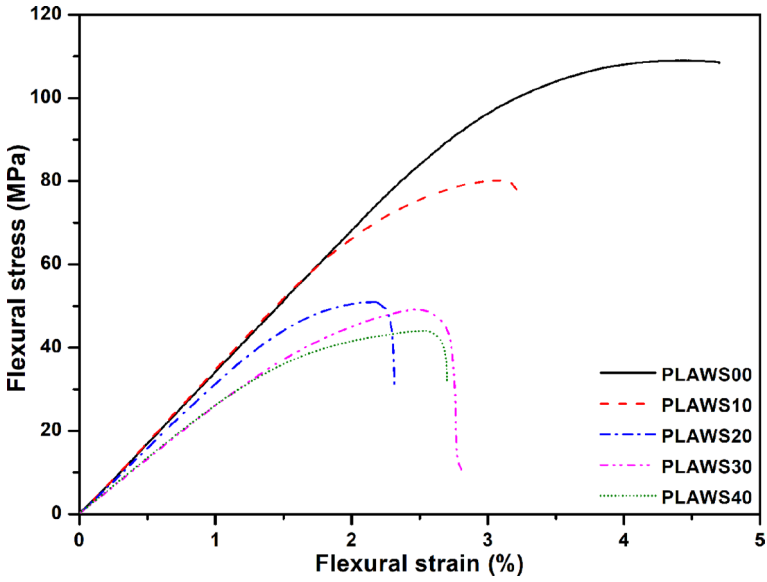
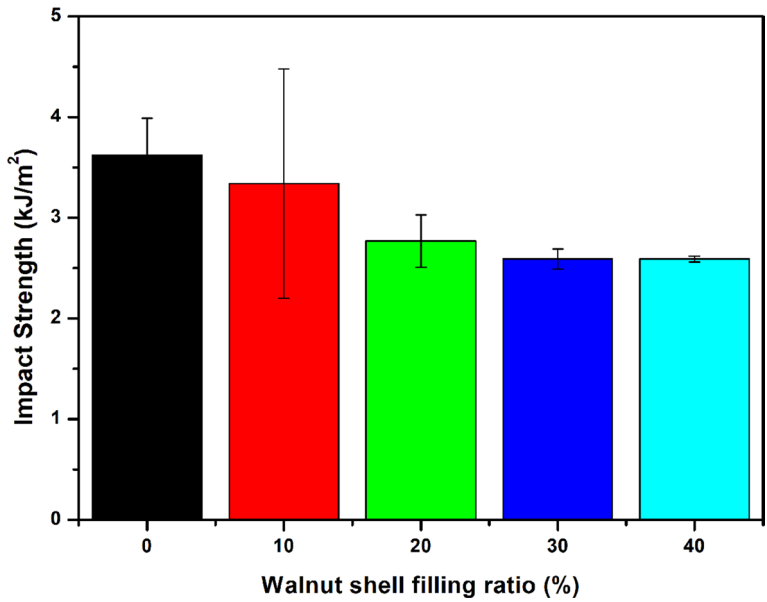**Fig. 3** Graphical comparison of three-point bending test results for PLA/WS composites

Fig. 4 Graphical comparison of Izod impact test results for PLA/WS composites

Izod impact test results of PLA/WS composites

The results of the Izod impact test are graphically compared in Fig. 4. According to the obtained results, pure PLA with the code PLAWS00 demonstrates the highest impact strength. In comparison, sample PLAWS10 exhibits a slightly lower impact strength when compared to pure PLA, with a considerably high standard deviation. This high standard deviation indicates variability in the results, which could be attributed to either the homogeneous distribution of walnut shell within the composite structure or the interface between PLA and walnut shell. Sample PLAWS20 shows a moderate level of impact resistance with an acceptable standard deviation. Although the impact strength between samples PLAWS30 and PLAWS40 is similar, PLAWS40 has a lower standard deviation, indicating more consistent results. Overall, in terms of material selection and design, pure PLA (PLAWS00) demonstrates more stable impact resistance. The incorporation of biodegradable additives and mineral-based reinforcements into the composite, along with WS, can improve impact resistance [4].

Hardness test results of PLA/WS composites

The graphical comparison of Shore D hardness test results for PLA/WS composites is presented in Fig. 5. The highest hardness value was measured in pure PLA (82.6 Sh. D). When examining the standard deviation (0.55), it is observed that the hardness measurement results for pure PLA are quite stable. Sample PLAWS10, with a 10% WS filler ratio, presents a hardness value close to that of pure PLA (82.2 Shore
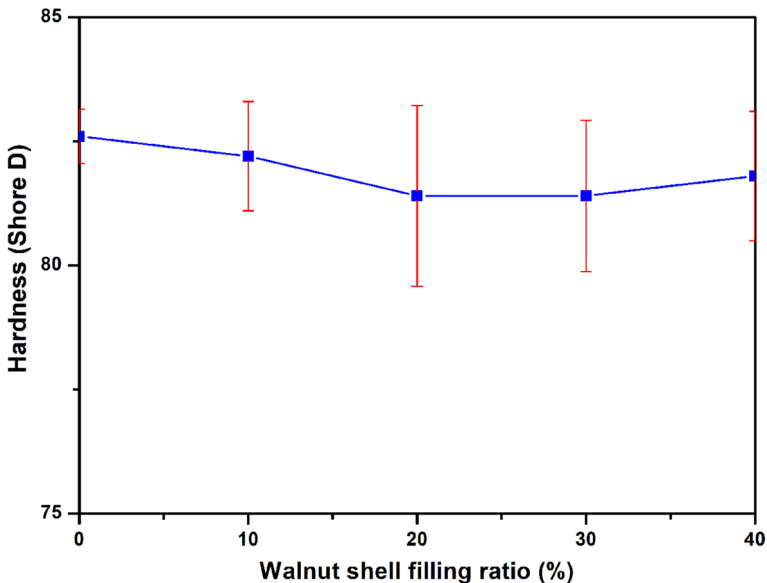

Fig. 5 Graphical comparison of hardness test results for PLA/WS composites

D), but with a considerably high standard deviation (1.10), indicating variability in the results. The hardness value of sample PLAWS20 is slightly lower than that of pure PLA (81.4 Shore D), and the results also show more variability (standard deviation 1.82). Samples PLAWS30 and PLAWS40 have similar hardness values (81.4 Shore D and 81.8 Shore D, respectively), but the hardness results for both samples are obtained with considerable variability (standard deviation 1.52 and 1.30). These results indicate that the surface hardness of sample PLAWS00 is the highest and most stable, while WS-filled samples exhibit lower hardness and more variable results. Overall, there are no significant differences in hardness between pure PLA and WS-filled samples. The higher standard deviation in WS-filled samples is thought to be influenced by the distribution of WS within the structure at the measurement point, resulting in voids and interfaces.

Density measurement results of PLA/WS composites

The density measurement results are presented in Fig. 6. Upon examining the densities of PLA/WS composites, it is evident that the density of the composite material decreases with the filler ratio. This observation can be attributed to the lower density of the walnut shell used as the filler material compared to PLA. The trajectory of the density curve shown in Fig. 6 does not exhibit a linear pattern with increasing filler ratio. This can be attributed to the relatively reduced homogeneous distribution of WS within the structure as the filler ratio increases, leading to the formation of air voids [43], consequently affecting the decrease in the composite density. The obtained results suggest that the physical properties of composite materials can vary
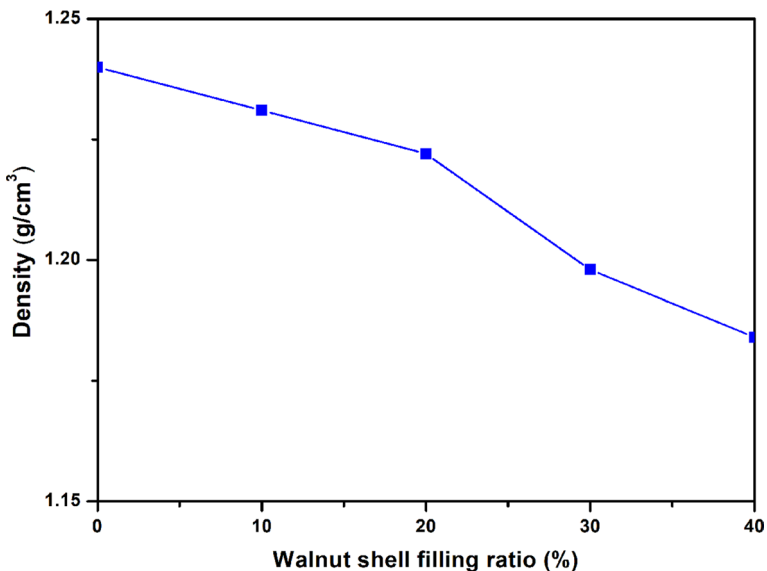

Fig. 6 Graphical comparison of density measurement results for PLA/WS composites

based on the filler ratio. Changes in the density of PLA/WS composites, whether upward or downward, can positively impact the alteration of the material's mechanical strength and thermal properties when additional additives such as compatibilizers or chain extenders are utilized in the compounds [44, 45]. These composite materials, characterized by their lightweight nature and simultaneously high density, hold potential for various industrial applications. These findings significantly contribute to our understanding of how biodegradable materials and natural filler materials can be utilized in composite material production and the direction in which their densities evolve.

Water absorption test results of PLA/WS composites

The time-dependent water absorption capacities of both PLA and PLA/WS composites are illustrated in Fig. 7. The water absorption capacity of pure PLA is lower compared to that of PLA/WS composites. The primary contributor to the heightened water absorption capacity in PLA composites is believed to be the hemicellulose present in WS. This is due to cellulose, with its resistant molecular structure and naturally formed hydrogen bonds, keeping the water absorption capacity at a low level. However, hemicellulose is more hydrophilic than cellulose, leading to an increased water absorption capacity in the composites. In all PLA/WS composites except pure PLA, degradation initiates after 192 h. Evaluations within the PLA/WS composites indicate that as the WS filler ratio increases, the initially high-water absorption capacity starts to decrease after 96 h. This phenomenon can be associated with the increased WS filler ratio limiting swelling
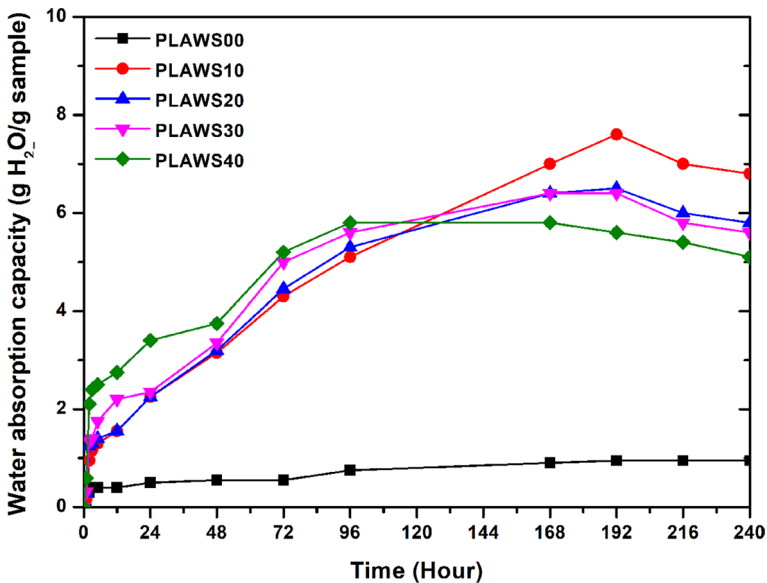

Fig. 7 Graphical comparison of water absorption capacity for PLA/WS composites

in the particles and preventing more water entry into the structure. This increase is likely due to the hydrophilic nature of the filler material, a phenomenon supported by similar findings in the literature [46, 47].

FT-IR test results of PLA/WS composites

The FT-IR spectra of WS, PLA, and PLA/WS composites are presented in Fig. 8. In the FT-IR spectrum of pure WS (Fig. 8), distinct peaks are observed, including O–H stretching at 3350 cm^{-1}, aliphatic C–H stretching at 2930 cm^{-1}, carbonyl C=O stretching of carboxylic groups in hemicelluloses and pectin at 1740 cm^{-1}, aromatic C=C stretching at 1596 and 1507 cm^{-1}, aliphatic C–H stretching at 1462 and 1373 cm^{-1}, C–H aromatic ring vibration at 1423 cm^{-1}, and C–O stretching of acetyl groups in lignin at 1240 cm^{-1}. In the FT-IR spectrum of pure PLA, noticeable peaks include CH_3-derived C–H stretching at 2997 and 2947 cm^{-1}, a carbonyl C=O peak at 1750 cm^{-1}, C–H stretching of methylol groups at 1451 and 1360 cm^{-1}, and C–O stretching frequency at 1180 and 1080 cm^{-1}. Upon examining the FT-IR spectra of PLA/WS composites with different WS ratios, it can be generally stated that their structures are similar. As the WS ratio increases in PLA/WS composites, the O–H band becomes more pronounced, widens, and shifts to slightly lower wavenumbers. This is believed to be attributed to the formation of hydrogen bonds by the free hydroxyl groups in the environment [48].
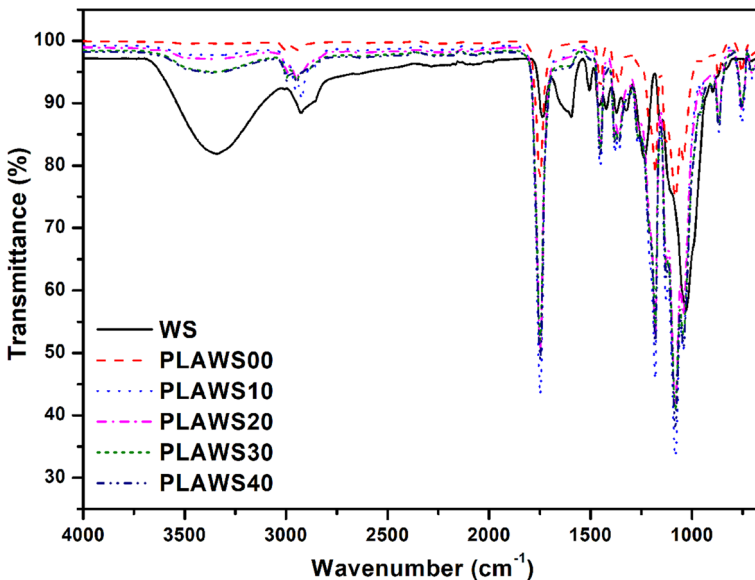

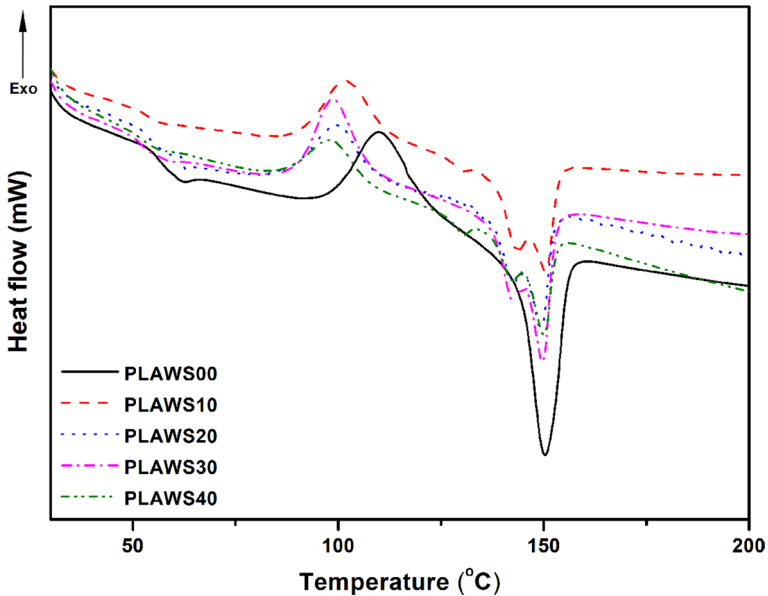**Fig. 8** Graphical comparison of FT-IR spectrum for PLA/WS composites

Fig. 9 DSC curves of PLA/WS composites

Table 4 The numerical data obtained from the DSC test

Code	T_g (°C)	T_{cc} (°C)	T_m (°C)	$(\Delta H_m - \Delta H_{cc})$ (J/g)	Xc (%)
PLAWS00	57.5	109.8	150.4	4.4	4.7
PLAWS10	54.0	101.6	150.4	4.2	5.0
PLAWS20	62.8	99.9	149.1	4.7	6.3
PLAWS30	52.3	98.5	149.6	5.7	8.8
PLAWS40	53.5	97.8	150.0	2.3	4.1

DSC test results of PLA/WS composites

The DSC analysis aimed to assess the impact of Tg (glass transition temperature), Tcc (cold crystallization temperature), Tm (melting temperature), and crystallinity on the composites. In this study, data from the initial heating cycle, offering insights into the structure obtained solely from the injection molding process, were presented. As depicted in the DSC curves in Fig. 9 and summarized in Table 4, the glass transition temperature exhibited no significant changes for both pure PLA and PLA/WS composites. Even composites with higher WS content remained within the limits specified by the polymer producer for the glass transition temperature. Regarding the cold crystallization temperature, a slight shift towards lower temperatures was observed from pure PLA towards the composites. Concerning the melting temperature, double peaks for the melting endotherm were observed, potentially

explained by the melting of crystallites of different sizes and/or the quality of the order. Data related to the crystallinity of the materials indicated that the addition of WS to the PLA matrix increased crystallinity, but it did not exert a very pronounced effect on this property. This result suggested that the difference in enthalpies was small, signifying that WS had a much smaller impact on crystallinity (all composites maintained very low crystallinity ratios) [42, 49].
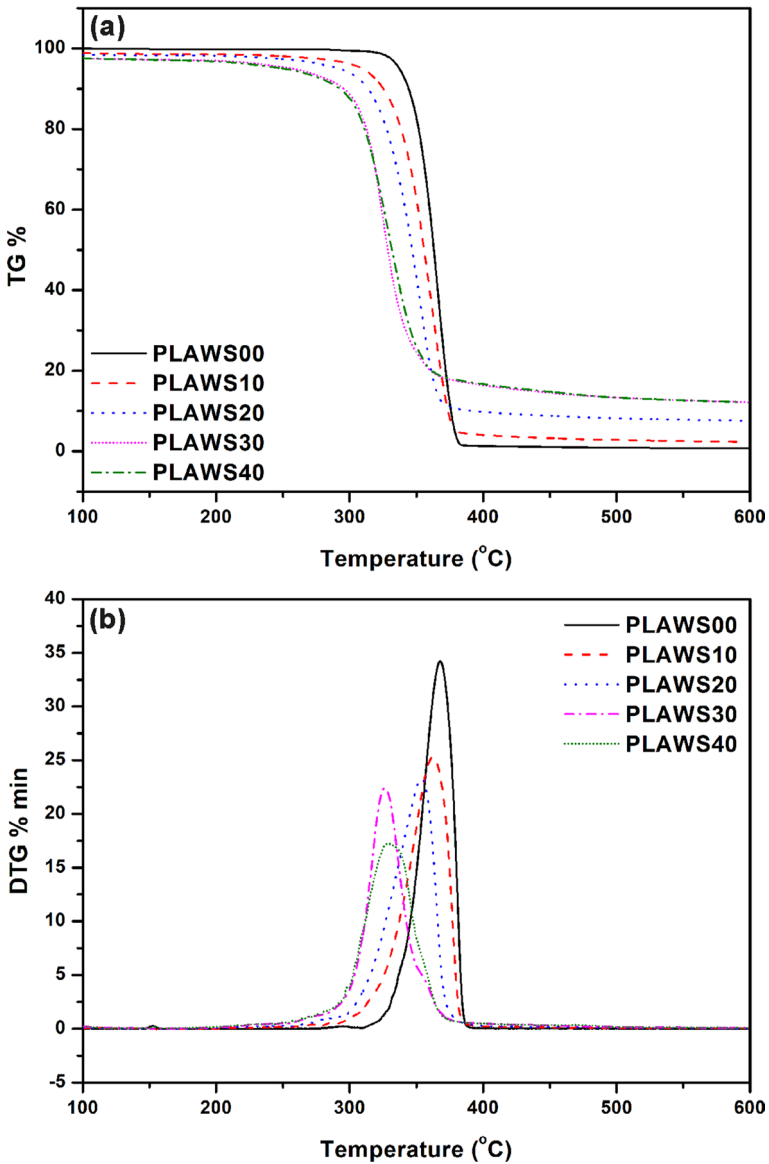

Fig. 10 TGA curves of PLA/WS composites **a** TG and **b** DTG

Table 5 The numerical data obtained from the TGA test

Code	T_5 (°C)	T_{50} (°C)	T_{max} (°C)	Residue at 600 °C (%)
PLAWS00	341.3	367.6	384.3	0.7
PLAWS10	323.7	362.2	382.8	2.3
PLAWS20	313.5	353.6	370.2	7.6
PLAWS30	301.2	326.4	350.2	12.1
PLAWS40	300.5	328.4	359.1	12.1

TGA test results of PLA/WS composites

The thermal stability of PLA and PLA/WS composites is illustrated in Fig. 10, and the numerical data for the TGA test are provided in Table 5. All samples exhibit a simple thermal degradation step in the weight loss curves between 250 and 400 °C. The addition of WS adversely affects thermal stability, evident in the leftward (lower) shift of the weight loss temperature in PLA/WS composites compared to pure PLA. This divergence can be attributed to the degradation of the total cellulose content of WS with some lignin, which is associated with PLA proliferation. This is because the addition of thermally sensitive cellulose material to PLA is known to reduce the thermal stability of pure PLA, especially at higher processing temperatures [49]. A possible reason for this could be related to the absorption of water on the surface of PLA/WS composites. These active regions on the surface might also act as depolymerization catalysts, accelerating the degradation of PLA. All these activities may contribute to a decrease in the molecular weight of PLA in PLA/WS composites, thereby promoting PLA degradation. Generally, an increase in the WS ratio reduces thermal stability and increases the amount of solid residue (Residue at 600 °C). With the increase in WS, thermal degradation initiates at lower temperatures (T5). The loss of half of the initial weight (T50) and the peak temperature of thermal degradation (Tmax) occur at lower temperatures in PLA/WS composites compared to pure PLA. Despite the acceleration of PLA's thermal degradation due to the addition of WS, it can still meet the required temperature range for injection molding and filament production (180–225 °C).

SEM microstructure imaging results of PLA/WS composites

Figure 11a depicts ground WS. The image reveals the fibrous and layered structure of the WS, prominently displaying its characteristics. Despite having a rough surface and fibrous structure, WS particles exhibit a spherical-like shape, characterized by their resemblance to spherical particles [50]. In the SEM images of pure PLA in Fig. 11b, the surface of the PLA sample appears quite smooth and exhibits a homogeneous structure. This smooth surface indicates that PLA is produced in a homogeneous manner, with low potential for defects or contamination. Additionally, as observed in Fig. 11b, the fracture surface of pure PLA shows less plastic
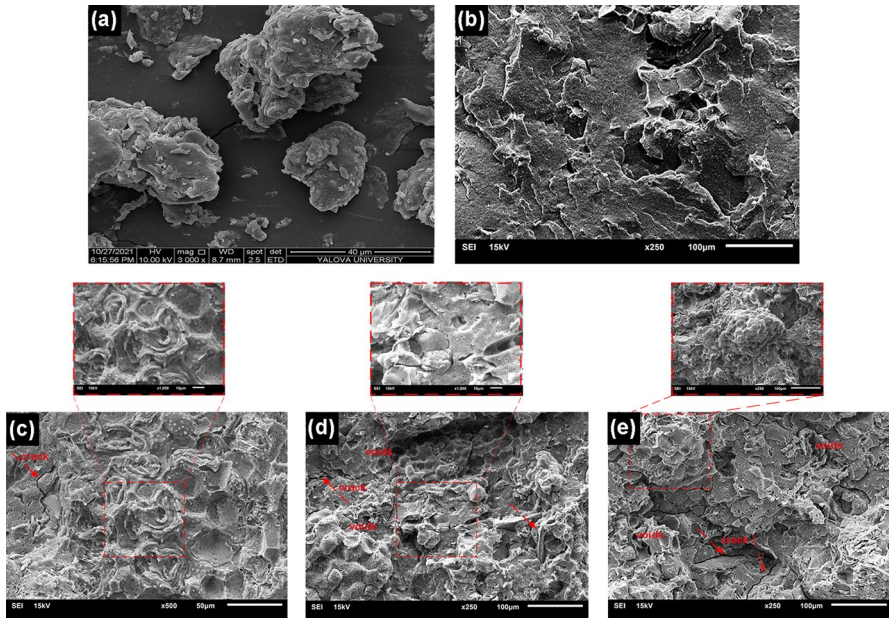
Fig. 11 SEM microstructure images: **a** walnut shell, **b** PLAWS00, **c** PLAWS10, **d** PLAWS20, **e** PLAWS40

deformation, giving the impression of a more brittle appearance. Figure 11c shows the SEM microstructure image of a PLA composite filled with 10% WS, Fig. 11d shows the SEM microstructure image of a PLA composite filled with 20% WS, and Fig. 11e shows the SEM microstructure image of a PLA composite filled with 40% WS. The structural features of WS-filled PLA composites have been examined in detail in these images. According to the results obtained from SEM images, WS particles are uniformly distributed in the melt without agglomeration. However, as the WS filler ratio increases, it is determined that the material becomes more brittle, and impact resistance properties decrease. With an increasing WS filler ratio, the interaction between WS and PLA matrix weakens, leading to the formation of voids in the composite structure. Fracture surfaces of PLA/WS composites are observed to be rough, which is thought to be due to the incomplete wetting of WS surfaces by the PLA matrix, contributing to the formation of voids in the composite structure [4, 46]. Additionally, SEM microstructure images clearly show that WS are detached from the fractured surfaces under impact, which is identified as a significant factor affecting the impact resistance and surface integrity of the composite.

Conclusion

In this study, the mechanical and thermal properties of PLA/WS composites with varying ratios of WS content, where no chemical treatment such as alkaline and silane has been applied, were experimentally investigated. The experimental

findings reveal that an increase in the WS filler ratio within PLA composites leads to a noticeable decline in various mechanical properties, including tensile strength, flexural strength, and impact resistance. The addition of WS has decreased the tensile strength of the PLA/WS composite by 32–65%, the flexural strength by 27–58%, the tensile modulus by 28%, and the flexural modulus by 22%, depending on the filler content. These results indicate a lower overall performance compared to pure PLA. While density shows a decrease with the WS filler ratio, the water absorption capacity exhibits a time-dependent pattern, characterized by initial increases followed by subsequent decreases. The highest water absorption capacity was measured after 192 h at a 10% WS filler ratio. An increase in the WS filler ratio resulted in a decrease in water absorption capacity, likely due to the filler's ability to limit swelling and prevent excess water ingress into the structure. The FT-IR analysis suggests structural similarities in PLA/WS composites, with observable shifts in the O–H band attributed to the formation of hydrogen bonds. DSC results indicate minimal impact on the glass transition temperature and crystallinity, while TGA reveals a reduction in thermal stability with higher WS content. The highest crystallization rate, measured at 8.8%, was observed in the composite coded as PLAWS30, with a WS filler content of 30%. The TGA test revealed complete degradation of all samples between 320 and 370 °C. SEM microstructure imaging highlights the uniform distribution of WS particles but underscores increased brittleness and reduced impact resistance with higher filler ratios. In conclusion, this study offers valuable insights into the effects of WS fillers on PLA composites, emphasizing the necessity for a meticulous consideration of filler ratios to strike a balance between enhanced sustainability and maintained mechanical performance.

Declarations

References

1. Barczewski M, Sałasińska K, Szulc J (2019) Application of sunflower husk, hazelnut shell and walnut shell as waste agricultural fillers for epoxy-based composites: a study into mechanical behavior related to structural and rheological properties. Polym Test 75:1–11
2. Cakir Yigit N, Karagoz I (2023) A review of recent advances in bio-based polymer composite filaments for 3D printing. Polym-Plast Technol Mater 62(9):1077–1095
3. Taib NAAB, Rahman MR, Huda D, Kuok KK, Hamdan S, Bakri MKB, Julaihi MRMB, Khan A (2023) A review on poly lactic acid (PLA) as a biodegradable polymer. Polym Bull 80(2):1179–1213
4. Lohar DV, Nikalje AM, Damle PG (2023) Synthesis and characterization of PLA hybrid composites using bio waste fillers. Mater Today: Proc 72:2155–2162
5. Saheb DN, Jog JP (1999) Natural fiber polymer composites: a review. Adv Polym Technol: J Polym Process Inst 18(4):351–363
6. Abraham E, Elbi PA, Deepa B, Jyotishkumar P, Pothen LA, Narine SS, Thomas S (2012) X-ray diffraction and biodegradation analysis of green composites of natural rubber/nanocellulose. Polym Degrad Stab 97:2378–2387
7. Suriapparao DV, Ojha DK, Ray T, Vinu R (2014) Kinetic analysis of co-pyrolysis of cellulose and polypropylene. J Therm Anal Calorim 117:1441–1451
8. Low JH, Andenan N, Rahman WAWA, Rusman R, Majid RA (2017) Evaluation of rice straw as natural filler for injection molded high density polyethylene biocomposite materials. Chem Eng 56:1081–1086. https://doi.org/10.3303/CET1756181
9. Bagherinia MA, Sheydaei M, Giahi M (2017) Graphene oxide as a compatibilizer for polyvinyl chloride/rice straw composites. J Polym Eng 37:661–670. https://doi.org/10.1515/polyeng-2016-0249
10. Brzyski P, Barnat-hunek D, Fic S, Szeląg M (2017) Hydrophobization of lime composites with lignocellulosic raw materials from flax hydrophobization of lime composites with lignocellulosic raw materials from flax. J Nat Fibers 14:609–620. https://doi.org/10.1080/15440478.2016.1250024
11. Nuñez AJ, Sturm PC, Kenny JM, Aranguren MI, Marcovich NE, Reboredo MM (2003) Mechanical characterization of polypropylene-wood flour composites. J Appl Polym Sci 88:1420–1428
12. Aranguren MI, Reboredo MM, Demma G, Kenny J (1999) Oak sawdust and hazelnut shells as fillers for a polyester thermoset. Holz als Roh- und Werkstoff 57:325–330
13. Oladele IO, Ibrahim IO, Akinwekomi AD, Talabi SI (2019) Effect of mercerization on the mechanical and thermal response of hybrid bagasse fiber/CaCO$_3$ reinforced polypropylene composites. Polym Test 76:192–198
14. Basboga İH, Atar İ, Karakus K, Mengeloglu F (2017) Determination of selected properties of PP based composites filled aggplant (Solanum melongena) stalks. Pro Ligno 13(4):276–282
15. Tufan M, Ayrılmış N (2016) Potential use of hazelnut husk in recycled high-density polyethylene composites. Bio Resour 11(3):7476–7489
16. Demirer H, Kartal İ, Yıldırım A, Büyükkaya K (2018) The utilisability of ground hazelnut shell as filler in polypropylene composites. Acta Phys Pol, A 134(1):254–256
17. Aydinli B, Çağlar A (2012) The investigation of the effects of two different polymers and three catalysts on pyrolysis of hazelnut shell. Fuel Process Technol 93:1–7
18. Balart JF, Fombuena V, Fenollar O, Boronat I, Nacher LS (2015) Processing and characterization of high environmental efficiency composites based on PLA and hazelnut shell flour (HSF) with biobased plasticizers derived from epoxidized linseed oil (ELO). Compos B. https://doi.org/10.1016/J.compositesb.2015.09.063
19. Salasinska K, Ryszkowska J (2012) Natural fibre composites from polyethylene waste and hazelnut shell: dimensional stability, physical, mechanical and thermal properties. Compos Interfaces 19(5):321–332. https://doi.org/10.1080/15685543.2012.726156
20. Barczewski M, Sałasińska K, Szulc J (2019) Application of sunflower husk, hazelnut shell and walnut shell as waste agricultural fillers for epoxy-based composites: a study into mechanical behavior related to structural and rheological properties. Polym Test 75:1–11
21. Essabir H, Nekhlaoui S, Malha M, Bensalah MO, Arrakhiz FZ, Qaiss A, Bouhfid R (2013) Biocomposites based on polypropylene reinforced with almond shells particles: mechanical and thermal properties. Mater Des. https://doi.org/10.1016/j.matdes.2013.04.031

22. Battegazzore D, Bocchini S, Alongi J, Frache A (2014) Plasticizers, antioxidants and reinforcement fillers from hazelnut skin and cocoa by-products: extraction and use PLA and PP. Polym Degrad Stab 108:297–306

23. Ramakrishna G, Purushothaman K, Sivakumar ER, Sreenivasan M (2021) An analysis on natural fiber composite materials. Mater Today: Proc 45:6794–6799

24. Catto AL, Stefani BV, Ribeiro VF, Santana RMC (2014) Influence of coupling agent in compatibility of post-consumer HDPE in thermoplastic composites reinforced with eucalyptus fiber. Mater Res 17(1):203–209

25. Ribeiro GL, Gandara M, Moreno DDP, Saron C (2017) Low-density polyethylene/sugarcane fiber composites from recycled polymer and treated fiber by steam explosion. J Nat Fibers. https://doi.org/10.1080/15440478.2017

26. Polat K (2017) Low-cost and high-capacity dye remover: a study of methylene blue adsorption by a thermoplastic elastomer blend system. Water Air Soil Pollut 228(9):329

27. Sadhukhan AK, Gupta P, Goyal T, Saha RK (2008) Modelling of pyrolysis of coal-biomass blends using thermogravimetric analysis. Biores Technol 99:8022–8026

28. Kufel A, Kuciel S (2020) Hybrid composites based on polypropylene with basalt/hazelnut shell fillers: the influence of temperature, thermal aging, and water absorption on mechanical properties. Polymers. https://doi.org/10.3390/polym12010018

29. La Mantia FP, Morreale M (2011) Green composites: a brief review. Compos A 42:579–588

30. Orue A, Eceiza A, Arbelaiz A (2020) The use of alkali treated walnut shells as filler in plasticized poly (lactic acid) matrix composites. Ind Crops Prod 145:111993

31. Umerah CO, Kodali D, Head S, Jeelani S, Rangari VK (2020) Synthesis of carbon from waste coconutshell and their application as filler in bioplast polymer filaments for 3D printing. Compos B Eng 202:108428

32. Lendvai L, Singh T, Fekete G, Patnaik A, Dogossy A (2021) Utilization of waste marble dust in poly (lactic acid)-based biocomposites: mechanical, thermal and wear properties. J Polym Environ 29:2952–2963

33. Calì M, Pascoletti G, Gaeta M, Milazzo G, Ambu R (2020) New filaments with natural fillers for FDM 3D printing and their applications in biomedical field. Proc Manufact 51:698–703

34. Calì M, Pascoletti G, Gaeta M, Milazzo G, Ambu R (2020) A new generation of bio-composite thermoplastic filaments for a more sustainable design of parts manufactured by FDM. Appl Sci 10(17):5852

35. Fouladi MH, Namasivayam SN, Sekar V, Marappan P, Choo HL, Ong TK, Baniotopoulos C (2020) Pretreatment studies and characterization of bio-degradable and 3d-printable filaments from coconut waste. Int J Nanoelectron Mater 13:137–148

36. da Silva SM, Oliveira JM (2018) Cork-polylactide composites reinforced with polyhydroxyalkanoates for additive manufacturing. In: 18th European conference on composite matererials, Athens, Greece

37. Sekar V, Zarrouq M, Namasivayam SN (2021) Development and characterization of oil palm empty fruit bunch fibre reinforced polylactic acid filaments for fused deposition modelling. J Mech Eng (JMechE) 8(1):89–107

38. Yu W, Dong L, Lei W, Zhou Y, Pu Y, Zhang X (2021) Effects of rice straw powder (RSP) size and pretreatment on properties of FDM 3D-printed RSP/poly (lactic acid) biocomposites. Molecules 26(11):3234

39. Kumar AM, Jayakumar K (2022) Mechanical and drilling characterization of biodegradable PLA particulate green composites. J Chin Inst Eng 45(5):437–452

40. Kuan HTN, Tan MY, Shen Y, Yahya MY (2021) Mechanical properties of particulate organic natural filler-reinforced polymer composite: a review. Compos Adv Mater 30:26349833211007504

41. Alpár T, Markó G, Koroknai L (2017) Natural fiber reinforced PLA composites: effect of shape of fiber elements on properties of composites. Handb Compos Renew Mater 2:287–309

42. Rabelo LH, Munhoz RA, Marini J, Maestrelli SC (2021) Development and characterization of PLA composites with high contents of a Brazilian refractory clay and improved fire performance. Mater Res 25:e20210444

43. Gutiérrez TJ, Ollier R, Alvarez VA (2018) Surface properties of thermoplastic starch materials reinforced with natural fillers. In: Thakur V, Thakur M (eds) Functional biopolymers. Springer Series on polymer and composite materials. Springer, Cham. https://doi.org/10.1007/978-3-319-66417-0_5

44. Ghalia MA, Dahman Y (2017) Investigating the effect of multi-functional chain extenders on PLA/PEG copolymer properties. Int J Biol Macromol 95:494–504

45. Zhao X, Pelfrey A, Pellicciotti A, Koelling K, Vodovotz Y (2023) Synergistic effects of chain extenders and natural rubber on PLA thermal, rheological, mechanical and barrier properties. Polymer 269:125712
46. Mahmoud Y, Belhanche-Bensemra N, Safidine Z (2022) Impact of microcrystalline cellulose extracted from walnut and apricots shells on the biodegradability of Poly (lactic acid). Front Mater 9:1005387. https://doi.org/10.3389/fmats.2022.1005387
47. Moo-Tun NM, Iñiguez-Covarrubias G, Valadez-Gonzalez Y (2020) Assessing the effect of PLA, cellulose microfibers and CaCO$_3$ on the properties of starch-based foams using a factorial design. Polym Test 86:106482. https://doi.org/10.1016/j.polymertesting.2020.106482
48. Çakır Yiğit N, Karagöz İ (2021) Ceviz Kabuğu Esaslı Polilaktik Asit (PLA) Kompozit Filamentlerin Hazırlanması ve Karakterizasyonu. In: 9th international fiber and polymer research symposium, 19–20 Kasım Uşak, Türkiye, pp 51–58
49. Altun M, Celebi M, Ovali S (2022) Preparation of the pistachio shell reinforced PLA biocomposites: effect of filler treatment and PLA maleation. J Thermoplast Compos Mater 35(9):1342–1357
50. Salasinska K, Barczewski M, Górny R, Kloziński A (2018) Evaluation of highly filled epoxy composites modified with walnut shell waste filler. Polym Bull 75:2511–2528. https://doi.org/10.1007/s00289-017-2163-3